




Research Article

Investigating the Influence of Bath Temperature on the Chemical Bath Deposition of Nanosynthesized Lead Selenide Thin Films for Photovoltaic Application

Saka Abel ¹, Jule Leta Tesfaye,^{1,2} Lamessa Gudata,¹ Fekede Lamessa,¹ Ramaswamy Shanmugam,³ L. Priyanka Dwarampudi,⁴ N. Nagaprasad ⁵, and Ramaswamy Krishnaraj ^{2,6}

¹Department of Physics, College of Natural and Computational Science, Dambi Dollo University, Ethiopia

²Centre for Excellence-Indigenous Knowledge, Innovative Technology Transfer and Entrepreneurship, Dambi Dollo University, Ethiopia

³TIFAC, CORE-HD, JSS College of Pharmacy, JSS Academy of Higher Education & Research, Ooty, Nilgiris, Tamil Nadu, India

⁴Department of Pharmacognosy, JSS College of Pharmacy, JSS Academy of Higher Education & Research, Ooty, Nilgiris, Tamil Nadu, India

⁵Department of Mechanical Engineering, ULTRA College of Engineering and Technology, Madurai, 625104 Tamilnadu, India

⁶Department of Mechanical Engineering, College of Engineering and Technology, Dambi Dollo University, Ethiopia

Correspondence should be addressed to Ramaswamy Krishnaraj; prof.dr.krishnaraj@dadu.edu.et

Received 2 August 2021; Accepted 24 January 2022; Published 9 February 2022

Academic Editor: A. Madhan Kumar

Copyright © 2022 Saka Abel et al. This is an open access article distributed under the Creative Commons Attribution License, which permits unrestricted use, distribution, and reproduction in any medium, provided the original work is properly cited.

Thin films of CBD are formed on metal surfaces from an aqueous solution containing $\text{Pb}(\text{NO}_3)_2$ and $\text{Na}_2\text{O}_4\text{Se}$. The impact of the bath temperature upon lead selenide NPs is analyzed. The evaluation of X-ray diffraction demonstrates that the produced NPs were polycrystalline with (111) orientation. The morphological analysis of the surface shows that the grains are spherical gemstones. As the bath temperature was raised from 20 to 85 degrees Celsius, the energy bandgap decreased from 2.4 to 1.2 eV, indicating a reduction in the band gap. Micron-sized nanoparticles produced at 85 degrees Celsius exhibited the best crystallinity and were uniformly spread across the surface of the substrate with excellent particle sizes. If the solution bath temperature increases from 20°C to 85°C, the average strength of PL decreases. The maximum photoluminescence strength is predominantly because of self-trapped exciton recombination, formed from O_2 vacancy and particle size called defect centers, for the deposited thin films at 45°C and 85°C. The photoluminescence intensity rises sequentially with all temperatures. Therefore, the finest solution temperature is 85 degrees Celsius.

1. Introduction

Currently, the world is in trouble of air pollution released from nonrenewable sources of energy such as coal, natural gas, fossil fuels, and fabrics [1]. A wide-ranging investigation has been dedicated to producing numerous kinds of semiconductor thin films which are applicable in renewable sources of energy like solar cells [2]. This is because of their potential uses in the production of photovoltaic materials, optical-electronic devices, sensors, and infrared indicator

instruments [3]. The lead selenide thin films appeal consideration of many scholars because they are low cost, exist in abundance, and retain semiconducting material goods [4, 5]. There have been numerous ways for the fabrication of thin films of lead selenide that have been discovered, which comprise electrodeposition, CBD, electrochemical atomic layer, photochemical, molecular beam epitaxial, and pulsed laser deposition method [6], amongst other techniques. Thin films created by chemical methods are frequently considerably costly than thin films produced by

capital-intensive physical techniques. CBD methods were specially picked for their several advantages, including their minimal price, broad area manufacturing, and ease of use in equipment setup [7]. Several other semiconductor thin films, notably [8–10] ZnS, have been successfully deposited using a chemical approach in the past few decades and also SnS, PbSe, CdSe, ZnSe, CdS, PbS, Cu₂S, CuInS, and CuBiS₂ on glass substrates [11–15], and they have no longer quality. There are very few chemically prepared lead selenide thin films reported by using glass substrates in an alkaline base. But this can make deletions of films and affect the quality of prepared films. They release hydroxide chemicals during their depositions [16–20]. For the present work, we have used metallic substrates to grow PbSe thin films by chemical bath deposition procedure in an acidic medium.

2. Materials and Methods

2.1. Materials and Fabrication of the Sample. Chemical bath deposition was used to deposit PbSe thin films on a metallic substrate (30 × 70 × 1 mm) using a chemical bath deposition process. Before depositing, the metal substrate was thoroughly washed in ethanol for 15 minutes after that, ultrasonically cleaned with a deionized solution for the next 20 minutes, and then finally desiccated in warm air. An aqueous solution of lead nitrate was used as a metallic precursor source that is lead, sodium selenite as the sulfide ion source, and [(HOC₂H₄)₃N] as a complexing agent for the synthesis of lead sulfide thin films [10, 11]. All of the chemicals that were used in the deposition were of analytical quality. Many of the treatments were made with deionized water as a base. In a step-by-step deposition procedure, 25 ml of 0.2 M lead nitrate was mixed with 10 ml of triethanolamine agent to form a complex. This has been followed by the addition of 15 milliliters of 0.2 M sodium selenite; the pH of the resulting mixture was adjusted to 4 by adding a droplet of sulfuric acid [12], and swirling it was gradually introduced to the reaction mixture constantly for several minutes. The clean metal substrates were produced in order to grow nanoparticles of lead selenide on the surface of the metal. The temperatures were 20°C, 45 degrees Celsius, and 85 degrees Celsius, respectively. After the deposition time of 95 min, we fetch the water from the chemical solution by using the syringe. The bottom of the glass of the bath solution is left with molten lead selenide nanoparticles. Next, the metal substrates were coated with molten lead selenide, and it was dried in the air, splashed with deionized water, and dehydrated in desiccators for even more analysis.

2.2. Characterization Methods. The crystalline geometries of the nanosynthesized PbSe thin films were investigated employing an X-ray diffraction (XRD) apparatus from PANalytical, model US [13], to determine their composition. The diffractometer was connected with a CuK source that operates at 35 kV and 23 mA; all scans were obtained in a 2θ range from 20 to 85°. An optical absorption measurement was executed using a Jeneway 6850 UV/visible spectrophotometer in the range from 226 to 2250 nm. The morphology of nanoparticles size was characterized by scanning

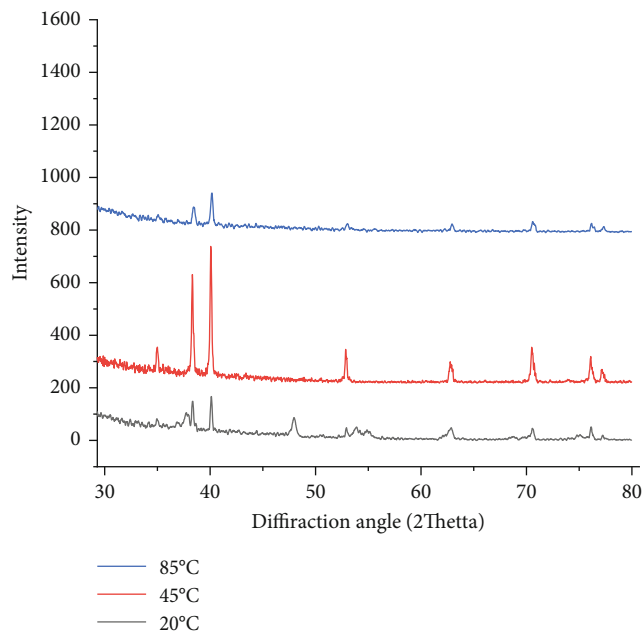


FIGURE 1: The XRD body of PbSe fine films formed at different bath temperatures: (1) 20°C, (2) 45°C, and (c) 85°C (lead selenide)

electron microscopy (SEM) in a Hitachi SU5000 with an operating voltage of 20 kV. Photoluminescence of the prepared material was analyzed by using a photoluminescence spectrophotometer.

3. Results and Discussion

Images of X-ray diffraction (XRD) structures of films deposited at different bath temperatures, including 20°C, 45°C, and 85°C, are shown in Figure 1. Exactly four peaks were observed on the film made at 45°C, which happened at $2\theta = 26.5^\circ$ and 29.6° . Raising bath temperature (to 85°C) enhanced the strength of the PbSe-related peaks, but only at the expense of the overall peak intensity. Diffraction across the (111) plane exhibits the maximum intensity with a well-defined sharp peak, suggesting that the material processed has a high degree of crystallinity. This suggests that when the temperature of the bath rises, the particle sizes of the thin film that is being deposited grow in proportion. When the bath temperature was raised, the number of PbSe peaks expanded as well. PbSe structure with (111) planes has been discovered, as indicated by the peaks that have been produced. Every one of these peaks, which corresponded to the cubic phase of lead diselenide, was a good match with the conventional data [12]. The values of the three lattice constants are all the same (6.128). Contrarily, it is the metal substrate that was utilized to conduct the analysis that is responsible for the occurrence of the Iron dioxide peak in the XRD pattern. At the 2θ values of 40.3, 52.8, and 67.3, four peaks were seen. Iron oxide has an orthorhombic structure, and the peaks indicated with solid triangles were connected with mirrors of the cubic structure of lead selenide, while the peaks indicated with undefended diamonds are related with reflections of the orthorhombic structure of lead

TABLE 1: Comparison of evaluated and standard “ d ” and 2θ values for nanosynthesized PbSe thin films with varied bath temperatures (20°C, 45°C, and 85°C) and deposition time at 95 minutes.

SI. No.	Bath temperature (°C)	Miller index (hkl) plane	2θ values	Lattice constants (Å)	Particle size (nm)
1	20	(111)	25.43	6.128	52.9
2	45	(222)	26.21	6.128	62.7
3	85	(444)	28.54	6.128	70.65

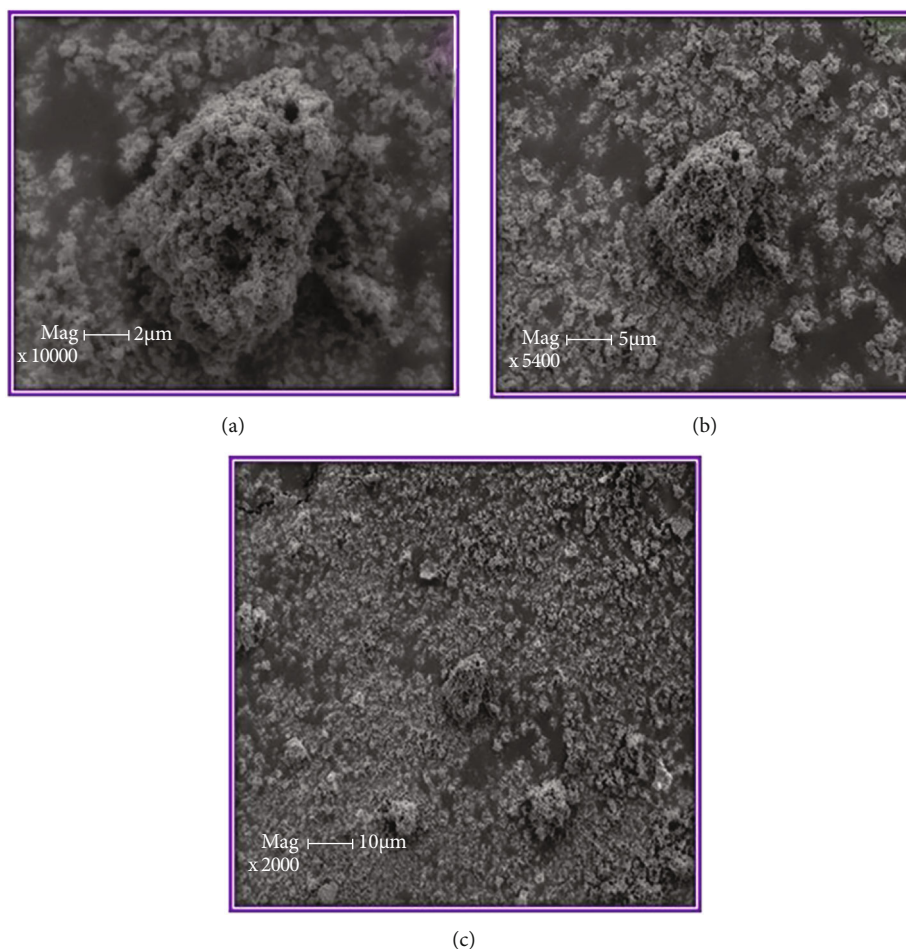


FIGURE 2: The scanning electron microscope micrograph of lead selenide thin films grown at different bath temperatures: (a) 20°C, (b) 45°C, and (c) 85°C.

selenide, and this result witnessed with scanning electron microscope analysis which is homogeneous with a cubic structure agrees with previous reports.

The size of the particle was premeditated by using Scherer’s formula; it is given by

$$D = \frac{0.9\lambda}{\beta \cos\theta}, \quad (1)$$

where λ shows wavelength, β stands for (FWHM) in rad, and θ represents the angle diffraction (Bragg angle). Comparison of evaluated and standard “ d ” and 2θ values for nanosynthesized PbSe thin films is listed in Table 1.

An investigation into the surface morphology of a film was conducted utilizing scanning electron microscopy (SEM). It can be used to determine the degree of grain and the architecture of produced films. The surface morphologies of the films produced at different bath temperatures ranging between 20 to 85 degrees Celsius are depicted in Figure 2. Every one of the samples was obtained at a voltage of 10.00 kV and a magnification of 20.71x. These were observed that the morphology of the samples changed in response to the bath temperature [14]. While all of the lead selenide thin films generated at all temperatures completely covered the metal substrates, the thin film deposited at 20°C is not relatively homogeneous and does not have excellent smoothness of the surface, as revealed by scanning

electron microscopy (Figure 2(a)). In these films, it was shown that the grains were extremely minute in size, with clearly defined grain borders between them. For the films deposited at 45°C and 85°C, well-defined grains can be seen in the images in Figure 2(b) and 2(c), respectively. The surfaces of the metal substrates were coated with a cubic-shaped PbSe crystal. PbSe surfaces grow more homogenous in appearance when the temperature of the bath is raised. Furthermore, it was shown that the grain amounts increased gradually. Once the tiny polycrystalline components have agglomerated together, they produce PbSe grains when heated to 85 degrees Celsius. The grains created a compact morphological characteristic across the substrate and had been tightly packed together in some way. In the present study, it was discovered that the temperature of the mixture played an important impact on the efficiency of the nanofabricated PbSe films.

The optical immersion of the nanosynthesized PbSe thin films deposited from different bath temperatures was measured in the wavelength with the range between 226 and 2250 nm, as shown in Figure 3. The absorbance of the films expressively raised when the bath temperature increased within the deliberated range of wavelength. The highest absorption of thin films was witnessed in the visible wavelength range. The optical absorption coefficient of the PbSe thin films was obtained from Lambert's equation:

$$\alpha = 2.30 \frac{A}{t}, \quad (2)$$

where A is the optical absorbance, α is the optical absorption coefficient, and t is the film thickness. The energy band gaps (E_g) of the PbSe thin films were calculated by utilizing Tauc's relation [18–25]:

$$(ah\nu)^n = k(h\nu - E_g), \quad (3)$$

where h is Planck's number, ν stands for frequency, k expresses the optical transition constant number, E_g is the energy of bandgap, and n is the transition type. The value of n is varying either 2 or 2/3 for direct allowed and forbidden transitions or 1/2 and 1/3 for indirect allowed and forbidden transitions, correspondingly [16]. The best linear fit for Equation (3) is given for $n = 2$ in the main absorption edge, representing that the thin films have direct optical band gaps. The $(ah\nu)$ axis intercept attained by extrapolating the linear portion of the $(ah\nu)^2$ vs. $(h\nu)$ curve gives the E_g of the films as shown in Figure 3. The E_g of the nanosynthesized PbSe thin films declined from 2.4 eV to 1.2 eV as the bath temperature of the solution increased from 20°C to 85°C. The decrease in bandgap could be due to the rise in the crystallite dimension with increasing the temperature in the deposition bath, and this result is the same as reported in [17]. The maximum absorbance in the visible light section and the band gaps of the thin films within the range 2.6 eV to 1.2 eV in all PbSe thin films provide the film's applicant materials as an absorber layer in photovoltaic thin-film solar cells as well as well-organized visible light photocatalyst [26–32].

Inappropriate to discover the optical study of deposited PbSe nanoparticles, photoluminescence was similarly used.

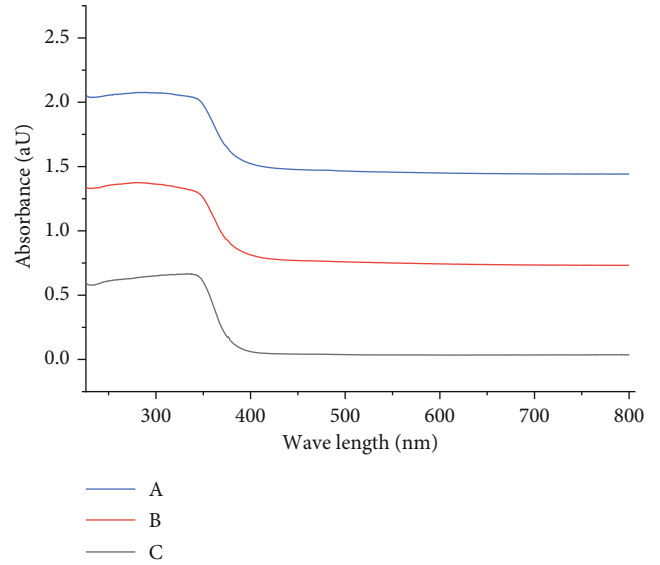


FIGURE 3: Plots of variation of optical absorption (αt) vs. wavelength film variation in bath temperatures: (a) 20°C, (b) 45°C, and (c) 85°C.

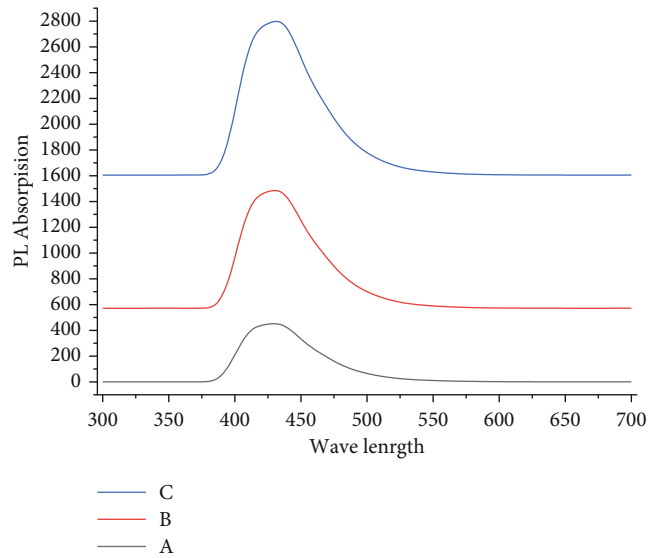


FIGURE 4: Photoluminescence spectra of lead selenide thin films deposited at different bath temperatures.

In the λ range from 350 nm to 600 nm at different temperatures, the PL spectra of the nanosynthesized thin films were reported. If the solution bath temperature increases from 20°C to 85°C, the average strength of PL decreases [19]. The maximum photoluminescence strength is predominantly because of self-trapped exciton recombination, formed from O_2 vacancy and particle size, which we call defect centers, for the deposited thin films at 45°C and 85°C. The photoluminescence intensity rises sequentially with all temperatures.

Figure 4 expresses that the absorption of nanosynthesized lead selenide thin films is formed at different bath temperatures. All the samples reveal a gradual rising absorbance

in the visible area, which provides the potential for these tools to be applicable in a photovoltaic solar cell. From the plotted figure, it shows that the samples synthesized at a greater temperature of the solution have greater absorption values related to other solution bath temperatures. Because of these, nanosynthesized thin films have the maximum uniform surface and well crystallinity thin films by comparing with other reported samples [19].

4. Conclusions

The creation of nanoproduced lead selenide (PbSe) thin films in acidic media can be accomplished with a simple and inexpensive chemical bath deposition process. It is expected that the chemical solution formed from lead nitrate and sodium selenate molecules will serve as a source of lead and selenide ions, respectively. The triethanolamine was served as a complexing mediator through deposition procedure. The X-ray diffraction pattern tells the creation of a cubic crystal structure with the toughest peaks ascribed to (111) miller index plane of lead selenide. PL confirmed that photoluminescence emission of the deposited thin films increased with increasing bath temperature. The deposited film at 85°C demonstrated excellent crystallinity and was evenly spread throughout the surface of the material with larger grain sizes. In response to an increment in bath temperature between 20°C to 85°C, the energy band gap narrowed, decreasing from 2.4 to 1.2 eV, making it acceptable for photovoltaic solar cells.

Data Availability

The data used to support the findings of this study are included within the article.

Disclosure

This study was performed as a part of the employment of the authors from Dambi Dollo University, Ethiopia.

Conflicts of Interest

The authors declare that there are no conflicts of interest.

References

- [1] S. Roa, M. Sandoval, and S. Suarez, "Rutherford backscattering spectroscopy analysis of the growth quality of chemical bath deposited PbSe thin films," *Solid State Sciences*, vol. 113, 2021.
- [2] S. Roa, M. Sandoval, M. J. C. Burgos, P. Manidurai, and S. Suarez, "Potential photovoltaic properties of thin film solar cells based on chemically deposited ZnO/PbSe junctions," *Journal of Alloys and Compounds*, vol. 871, 2021.
- [3] M. H. Jang, E. R. Hoglund, P. M. Litwin et al., "Photoconductive mechanism of IR-sensitive iodized PbSe thin films via strong hole-phonon interaction and minority carrier diffusion," *Applied Optics*, vol. 59, no. 33, pp. 10228–10235, 2020.
- [4] J. T. Harrison, E. Pantoja, M. H. Jang, and M. C. Gupta, "Laser sintered PbSe semiconductor thin films for mid-IR applications using nanocrystals," *Journal of Alloys and Compounds*, vol. 849, 2020.
- [5] C. K. Bando, I. Nkrumah, F. K. Ampong, R. K. Nkum, and F. Boakye, "Effect of annealing on the structure and optical properties of lead selenide and cadmium selenide thin film prepared by chemical bath deposition," *Chalcogenide Letters*, vol. 18, 2021.
- [6] B. B. Jin, S. Y. Kong, G. Q. Zhang et al., "Voltage-assisted SILAR deposition of CdSe quantum dots to construct a high performance of ZnS/CdSe/ZnS quantum dot-sensitized solar cells," *Journal of Colloid and Interface Science*, vol. 586, pp. 640–646, 2021.
- [7] I. A. Kariper, "Amorphous pbse thin film produced by chemical bath deposition at ph of 5–8," *Surface Review and Letters*, vol. 27, no. 4, 2020.
- [8] K. Ravi and V. Chitra, "Characteristics of lead selenide (PbSe) thin films deposited by CBD," *AIP Conference Proceedings*, vol. 2224, no. 1, 2020.
- [9] L. N. Maskaeva, V. M. Yurk, A. V. Belceva, I. V. Zarubin, A. D. Kutuyavina, and V. F. Markov, "Chemical bath synthesis of metal chalcogenide films. Part 42. Experimental verification of the deposition regions of PbSe by sodium selenosulfate and selenourea in the presence of various ligands," *Chemical Bath Synthesis of Metal Chalcogenide Films*, vol. 60, no. 10, pp. 88–98, 2019.
- [10] T. Hemati and B. Weng, "Experimental study of the size-dependent photoluminescence emission of CBD-grown PbSe nanocrystals on glass," *Nano Express*, vol. 1, no. 1, article 010030, 2020.
- [11] A. Kassim, H. S. Min, S. Monohorn, and S. Nagalingam, "Synthesis of PbSe thin film by chemical bath deposition and its characterization using XRD, SEM and UV-VIS spectrophotometer," *Makara Journal of Science*, vol. 14, no. 2, pp. 117–120, 2011.
- [12] A. Kassim, T. W. Tee, H. S. Min, S. Monohorn, and S. Nagalingam, "Effect of bath temperature on the chemical bath deposition of PbSe thin films," *Kathmandu University Journal of Science, Engineering and Technology*, vol. 6, no. 2, pp. 126–132, 2010.
- [13] S. Roa, M. Sandoval, and M. Sirena, "Chemical bath deposition of high structural and morphological quality PbSe thin films with potential optoelectronic properties for infrared detection applications," *Materials Chemistry and Physics*, vol. 264, 2021.
- [14] S. A. S. Peled, M. Perez, D. Meron et al., "Morphology control of perovskite films: a two-step, all solution process for conversion of lead selenide into methylammonium lead iodide," *Materials Chemistry Frontiers*, vol. 5, no. 3, pp. 1410–1417, 2021.
- [15] C. S. Diko, Y. Qu, Z. Henglin, Z. Li, N. A. Nahyoon, and S. Fan, "Biosynthesis and characterization of lead selenide semiconductor nanoparticles (PbSe NPs) and its antioxidant and photocatalytic activity," *Arabian Journal of Chemistry*, vol. 13, no. 11, pp. 8411–8423, 2020.
- [16] K. Ravi and V. Chitra, "Structural and surface morphology of lead selenide (PbSe) thin films," *IOP Conference Series: Materials Science and Engineering*, vol. 932, no. 1, 2020.
- [17] B. Yasabu and F. Gashaw, "Effect of sulfur ion concentration on structural and optical properties of lead sulfide thin films obtained by chemical bath deposition method," *International Journal of Agricultural and Natural Sciences*, vol. 14, no. 1, pp. 16–24, 2021.

- [18] R. Ahmed and M. C. Gupta, "Mid-infrared photoresponse of electrodeposited PbSe thin films by laser processing and sensitization," *Optics and Lasers in Engineering*, vol. 134, 2020.
- [19] M. C. Patino-Portela, P. A. Arciniegas-Grijalba, L. P. Mosquera-Sanchez et al., "Effect of method of synthesis on antifungal ability of ZnO nanoparticles: chemical route vs green route," *Advances in Nano Research*, vol. 10, no. 2, pp. 191–210, 2021.
- [20] S. Awan, K. Shahzadi, S. Javad, A. Tariq, A. Ahmad, and S. Ilyas, "A preliminary study of influence of zinc oxide nanoparticles on growth parameters of Brassica oleracea var italic," *Journal of the Saudi Society of Agricultural Sciences*, vol. 20, no. 1, pp. 18–24, 2021.
- [21] M. S. E. D. Salem, A. Y. Mahfouz, and R. M. Fathy, "The antibacterial and antihemolytic activities assessment of zinc oxide nanoparticles synthesized using plant extracts and gamma irradiation against the uro-pathogenic multidrug resistant *Proteus vulgaris*," *Biology of Metals*, vol. 34, no. 1, pp. 175–196, 2021.
- [22] T. Bhuyan, K. Mishra, M. Khanuja, R. Prasad, and A. Varma, "Biosynthesis of zinc oxide nanoparticles from *Azadirachta indica* for antibacterial and photocatalytic applications," *Materials Science in Semiconductor Processing*, vol. 32, pp. 55–61, 2015.
- [23] M. Raafat, A. S. El-Sayed, and M. T. El-Sayed, "Biosynthesis and anti-mycotoxigenic activity of Zingiber officinale Roscoe-derived metal nanoparticles," *Molecules*, vol. 26, no. 8, 2021.
- [24] A. Naseer, A. Ali, S. Ali et al., "Biogenic and eco-benign synthesis of platinum nanoparticles (Pt NPs) using plants aqueous extracts and biological derivatives: environmental, biological and catalytic applications," *Journal of Materials Research and Technology*, vol. 9, no. 4, pp. 9093–9107, 2020.
- [25] M. Asemani and N. Anarjan, "Green synthesis of copper oxide nanoparticles using Juglans regia leaf extract and assessment of their physico-chemical and biological properties," *Green Processing and Synthesis*, vol. 8, no. 1, pp. 557–567, 2019.
- [26] S. Ahmad, S. Munir, N. Zeb et al., "Green nanotechnology: a review on green synthesis of silver nanoparticles — an ecofriendly approach," *International Journal of Nanomedicine*, vol. 14, pp. 5087–5107, 2019.
- [27] R. Abbasian and H. Jafarizadeh-Malmiri, "Green approach in gold, silver and selenium nanoparticles using coffee bean extract," *Open Agriculture*, vol. 5, pp. 761–767, 2020.
- [28] S. Sarli, M. R. Kalani, and A. Moradi, "A potent and safer anticancer and antibacterial Taxus-Based green synthesized silver Nanoparticle," *International Journal of Nanomedicine*, vol. 15, pp. 3791–3801, 2020.
- [29] M. S. Jameel, A. A. Aziz, and M. A. Dheyab, "Green synthesis: proposed mechanism and factors influencing the synthesis of platinum nanoparticles," *Green Processing and Synthesis*, vol. 9, no. 1, pp. 386–398, 2020.
- [30] A. Banerjee, A. Sarkar, K. Acharya, and N. Chakraborty, "Nanotechnology: an emerging hope in crop improvement," *Nano Bio Science*, vol. 10, pp. 2784–2803, 2021.
- [31] S. Painuli, P. Semwal, A. Bachheti, R. K. Bachheti, and A. Husen, "Nanomaterials from non-wood forest products and their applications," *Nanomaterials for Agriculture and Forestry Applications*, pp. 15–40, 2020.
- [32] S. Abel, J. L. Tesfaye, R. Shanmugam et al., "Green synthesis and characterizations of zinc oxide (ZnO) nanoparticles using aqueous leaf extracts of coffee (*Coffea arabica*) and its application in environmental toxicity reduction," *Journal of Nanomaterials*, vol. 2021, Article ID 3413350, 6 pages, 2021.